The Effect of Inhomogeneous Surface Disorder on the Superheating Field of Superconducting RF Cavities

Vudtiwat Ngampruetikorn* and J. A. Sauls†

Center for Applied Physics & Superconducting Technologies

Department of Physics & Astronomy, Northwestern University, Evanston, IL 60208

Fermi National Accelerator Laboratory, Batavia IL, 60510-5011

(Dated: November 8, 2021)

Recent advances in surface treatments of Niobium superconducting radio frequency (SRF) cavities have led to substantially increased Q-factors and maximum surface field. This poses theoretical challenges to identify the mechanisms responsible for such performance enhancements. We report theoretical results for the effects of inhomogeneous surface disorder on the superheating field — the surface magnetic field above which the Meissner state is globally unstable. We find that inhomogeneous disorder, such as that introduced by infusion of Nitrogen into the surface layers of Niobium SRF cavities, can increase the superheating field above the maximum for superconductors in the clean limit or with homogeneously distributed disorder. Homogeneous disorder increases the penetration of screening current, but also suppresses the maximum supercurrent. Inhomogeneous disorder in the form of an impurity diffusion layer biases this trade-off by increasing the penetration of the screening currents into cleaner regions with larger critical currents, thus limiting the suppression of the screening current to a thin dirty region close to the surface. Our results suggest that the impurity diffusion layers play a role in enhancing the maximum accelerating gradient of Nitrogen treated Niobium SRF cavities.

Introduction — Type-II superconductors admit two thermodynamic phases in the presence of an external magnetic field H. The Meissner state is the equilibrium state for fields below a lower critical field $H < H_{c_1}$, while the Abrikosov state, characterized by the penetration of quantized flux into the bulk of the superconductor, is the thermodynamically stable phase for fields $H_{c_1} < H <$ H_{c_2} , where H_{c_2} is the critical field above which the superconductor becomes normal for any temperature $T \leq T_c$. Superconductors in the Meissner state exhibit perfect diamagnetism by generating an internal field, that exactly screens the external field. The source of the screening field is a dissipationless supercurrent, "screening current", confined to the vacuum-superconductor interface. The screening current penetrates into the superconductor over a mesoscopic length scale, the London penetration depth λ_L , which is sensitive to disorder. The magnitude of the screening current increases linearly with the applied field until the cost in kinetic energy of maintaining perfect diamagnetism is outweighed by the reduction in Gibbs energy via flux penetration into into the bulk. For type-II superconductors flux is quantized in units of $\Phi_0 = hc/2e$ and confined in tubes of radius of order the London penetration depth, and the lower critical field for flux penetration is $H_{c_1} = \Phi_0/2\pi\lambda_L^2$, which for SRF grade Nb is typically of order $H_{c_1} \approx 30 \, \mathrm{mT}$, or an accelerating field of $E_{\rm ac} \approx 25 \, {\rm MV/m}$.

Above H_{c_1} the Abrikosov state, with an array of quantized flux lines, is the thermodynamically stable phase. Motion of quantized flux generates Joule losses and is detrimental to to the performance of SRF cavities for particle acceleration. Understanding, and thus engineering, materials properties and physical processes governing the breakdown of the Meissner state is crucial for developing strategies to improve the performance of SRF cavities.

One key feature is that Meissner state can be maintained for fields higher than H_{c_1} as a meta-stable phase, made possible by a surface energy barrier to flux penetration [1]. At sufficiently high field, the so-called superheating field, $H_{\rm sh} > H_{c_1}$, the surface barrier vanishes, and quantized flux lines proliferate leading to dissipation

under RF excitation.

The superheating field depends on the geometry of the vacuum-superconductor interface as well as the spatial distribution of disorder within the region of the screening currents. For a planar half-space geometry the effects of homogeneous disorder and engineered multilayer superconductor-insulator structures has been studied [2– 6]. The main results are that homogeneous disorder increases the penetration depth, but reduces the critical current, with a modest enhancement of the superheating field at low temperatures [2]. The superheating field may be increased by introducing insulating layers to retard flux line penetration. Here we report results of a theoretical investigation of the effects of an impurity diffusion layer, i.e. a smoothly varying, coarse-grained impurity density within the region of the screening currents, on SRF cavities such as Nitrogen infused into Niobium [7].

In general it is technically challenging to obtain quantitative predictions for the superheating field as one must consider the stability of the Meissner state to inhomogeneous fluctuations of order parameter and charge currents, as well as nucleation of vortices around impurities, inclusions or sharp structures at the vacuumsuperconductor interface. Here we consider the upper limit for the superheating field, which is the lowest surface field at which the supercurrent density reaches the local critical current density at some point within the screening region near the vacuum-superconductor interface. This condition provides an upper bound to the superheating field since any increase in the local condensate momentum - equivalently the local vector potential - cannot increase the supercurrent density. At the superheating field the Meissner state is unstable to arbitrarily small perturbations of the order parameter and electromagnetic (EM) field. For extreme type-II superconductors, this approach is equivalent to the stability condition with respect to inhomogeneous fluctuations of order parameter and the associated EM response [8].

Type-II superconductors are characterized by Ginzburg-Landau (GL) parameter, $\kappa = \lambda_L/\xi \ge 1/\sqrt{2}$, where λ_L denotes the London penetration depth and

 ξ is the superconducting coherence length. Pure Nb is weakly type II with $\kappa \approx 1$. However, disorder leads to increased field penetration with $\kappa \gg 1$ in the "dirty limit", $\hbar/\tau \gg \Delta$, where τ is the mean quasiparticle-impurity collision time. In this strong type-II limit quasiparticles and Cooper pairs respond locally to a nearly uniform EM field.

Here we consider superconductors in the strong type-II limit occupying the half space x > 0 in the presence of an external magnetic field, $\mathbf{H}_{a} = H_{a}\hat{\mathbf{z}}$, applied parallel to the vacuum-superconductor interface. We include the effects of an impurity diffusion layer on the current response into the quasiparticle-impurity scattering rate and pairing self-energy. Based on Eilenberger's quasiclassical transport theory [9] we compute the superfluid momentum $\mathbf{p}_s = p_s(x)\hat{\mathbf{y}}$, screening supercurrent $\mathbf{j}_s = j_s(x)\hat{\mathbf{y}}$ and local magnetic induction $\mathbf{B} = B(x)\hat{\mathbf{z}}$ self-consistently. The superheating field $H_{\rm sh}$ is the value of the surface field, B(0), at which the supercurrent density reaches the local critical value anywhere in the screening region of the superconductor, i.e. $\min_x [j_c(x) - |j_s(x)|] = 0$. Note that the critical current density $j_c(x)$ is a function of position due to the inhomogeneous impurity diffusion layer.

Methods — For a superconductor in the strong type-II limit, with an impurity diffusion layer that also varies on a length scale much longer than ξ , we develop the Eilenberger transport equation as a perturbation expansion in the small ratios, $\epsilon \in \{\xi/\lambda_L, \xi/\zeta\}$, where ζ is the characteristic penetration length of the impurity diffusion layer (Appendix). To leading order in ϵ the current response is determined by the retarded quasiclassical propagator obtained from the homogeneous solution of the quasiclassical transport equation, but evaluated with the Doppler shifted excitation spectrum determined by the local condensate momentum, $p_s(x)$, and the local impurity self-energies, $\Sigma_{\rm imp}(x)$ and $\Delta_{\rm imp}(x)$,

$$\widehat{\mathfrak{G}}(\widehat{\mathbf{p}}, \varepsilon, x) = -\pi \frac{[\widetilde{\varepsilon}(\varepsilon, x) - \mathbf{v}_f \cdot \mathbf{p}_s(x)]\widehat{\tau}_3 - \widetilde{\Delta}(\varepsilon, x)(i\sigma_y\widehat{\tau}_1)}{\sqrt{|\widetilde{\Delta}(\varepsilon, x)|^2 - [\widetilde{\varepsilon}(\varepsilon, x) - \mathbf{v}_f \cdot \mathbf{p}_s(x)]^2}}$$

$$\equiv -\pi [\mathfrak{G}(\widehat{\mathbf{p}}, \varepsilon, x)\widehat{\tau}_3 - \mathfrak{F}(\widehat{\mathbf{p}}, \varepsilon, x)(i\sigma_y\widehat{\tau}_1)], \quad (1)$$

where $\hat{\tau}_i$ and σ_i denote the Pauli matrices in particle-hole and spin space, respectively, $\hat{\mathbf{p}}$ is the direction defined by a point on the Fermi surface, $\mathbf{p} = p_f \hat{\mathbf{p}}$, and $\mathbf{v}_f = v_f \hat{\mathbf{p}}$ is the corresponding Fermi velocity. In the absence of vortices the superfluid momentum can be related to the vector potential via $\mathbf{p}_s = (-e/c)\mathbf{A}$, where we have fixed the gauge by absorbing the gradient of the phase of the condensate into \mathbf{A} . The diagonal and off-diagonal propagators, \mathfrak{G} and \mathfrak{F} , encode the information about the local equilibrium quasiparticle and Cooper pair spectral functions.

The impurity renormalized quasiparticle excitation energy and off-diagonal pairing energy can then be expressed as

$$\tilde{\varepsilon}(\varepsilon, x) = \varepsilon + \gamma(x) \left\langle \mathfrak{G}(\hat{\mathbf{p}}, \varepsilon, x) \right\rangle_{\hat{\mathbf{p}}},
\tilde{\Delta}(\varepsilon, x) = \Delta(x) + \gamma(x) \left\langle \mathfrak{F}(\hat{\mathbf{p}}, \varepsilon, x) \right\rangle_{\hat{\mathbf{p}}},$$
(2)

 $\langle \ldots \rangle_{\hat{\mathbf{p}}}$ denotes an angular average over the Fermi surface and $\gamma(x)$ is the local impurity scattering rate. The order parameter, $\Delta(x)$, satisfies the mean-field BCS gap

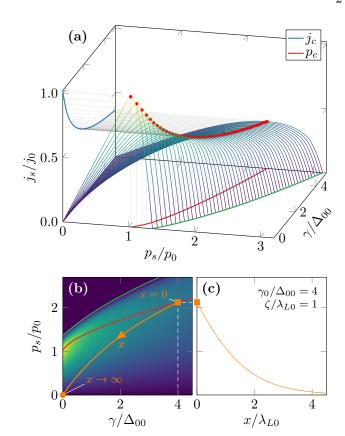


FIG. 1. Panel (a): the supercurrent density j_s as a function of condensate momentum p_s and impurity scattering rate γ at T=0. For fixed γ , the critical current, j_c , and condensate momentum, p_c , correspond to the values at which j_s is maximum (red filled circles). The critical current, j_c , decreases with increasing γ (blue line), whereas the critical condensate momentum, p_c , increases with increasing γ (red line). For $p_s > p_c$, the Meissner current is unstable. **Panel (b)**: a typical solution of Eq. (4) at the superheating field (orange curve), overlaid on a color density plot of j_s (same color scale as in (a)). The boundary conditions at x=0 and $x\to\infty$ are set by the superheating condition, $j_s(0) = j_c(0)$ (orange square) and the Meissner condition, $p_s(\infty) = 0$ (orange circle), respectively. The impurity scattering rate varies with x (arrow) based on Eq. (7) and vanishes as $x \to \infty$ (orange circle). Panel (c): spatial profile of the condensate momentum for the case shown in panel (b) with $\gamma_0/\Delta_{00}=4$ and $\zeta/\lambda_{L0}=1.$

equation,

$$\Delta(x) = \frac{g}{2} \oint d\varepsilon \tanh \frac{\varepsilon}{2T} \operatorname{Im} \langle f(\hat{\mathbf{p}}, \varepsilon, x) \rangle_{\hat{\mathbf{p}}}, \qquad (3)$$

where g is the pairing interaction, and the integration is extends over the low-energy bandwidth set by the Debye energy. The set of equations for the propagators, self energies, and mean-field gap equation are derived in the Appendix, including the next-to-leading order corrections from gradients of the leading order local propagators, which are smaller by a factor of order ϵ .

The solution for the field penetration into the inhomogeneous Meissner region of the superconductor is obtained from the local current response, which is in general a nonlinear function of the condensate momentum, $\mathbf{p}_s(x)$, combined with Ampère's equation. The latter equation can be expressed as

$$\partial_x^2 \mathbf{p}_s(x) - \frac{4\pi e}{c^2} \mathbf{j}_s[\mathbf{p}_s(x), \gamma(x)] = 0, \qquad (4)$$

where the supercurrent is obtained from the local solution for the quasiclassical propagator,

$$\mathbf{j}_s(x) = -eN_f \int d\varepsilon \tanh \frac{\varepsilon}{2T} \langle \mathbf{v}_f \, \mathcal{A}(\hat{\mathbf{p}}, \varepsilon, x) \rangle_{\hat{\mathbf{p}}} , \qquad (5)$$

where $N_f = p_f^2/2\pi^2\hbar^3v_f$ is the normal-state density of states, per spin, at the Fermi level. The Meissner current sums the charge current contributions from the states comprising both the negative energy condensate, as well as thermally excited Bogoliubov quasiparticles, governed by the angle-resolved spectral function, $\mathcal{A}(\hat{\mathbf{p}}, \varepsilon; x) \equiv \frac{-1}{\pi} \text{Im } \mathfrak{G}(\hat{\mathbf{p}}, \varepsilon; x)$, and the thermal distribution function, $\Phi(\varepsilon) = \tanh(\varepsilon/2T)$.

To determine the magnetic field distribution in the superconductor, we find the self-consistent condensate momentum distribution, $p_s(x)$, that determines the supercurrent, $j_s(x)$, given by Eq. (5), and is also the solution of Ampère's law given by Eq. (4). Ampère's law is also supplemented by boundary conditions at the surface and the asymptotic condition far from the vacuum-superconductor interface,

$$\nabla \times \mathbf{p}_s(x)|_{x=0} = (-e/c)\mathbf{H}_a$$
, and $\lim_{r \to \infty} \mathbf{p}_s(x) = 0$. (6)

The asymptotic condition reflects the fact that the Meissner state exhibits perfect diamagnetism. Equations (1)-(6) constitute a closed set of equations which are solved self-consistently. The local magnetic induction can then be computed directly from $\mathbf{B}(x) = (-c/e)\partial_x p_s(x)\hat{\mathbf{z}}$.

In order to determine the superheating field we first solve Eqs. (1)-(6) self-consistently for fixed temperature, T, external field, H_a , and impurity distribution, $\gamma(x)$, which yields the self-consistently determined spatial profiles for the condensate momentum, $p_s(x)$, and Meissner screening current, $j_s(x)$. The spatial profile of the magnetic field is obtained from the condensate momentum $B(x) = (-c/e)\partial_x p_s(x)$. To determine the superheating field, we determine the surface field, $B(0) = H_{\rm sh}$, at which the supercurrent and the superfluid momentum reach local critical values anywhere in the Meissner screening region.

Impurity Diffusion Layer — For concreteness we model the impurity diffusion layer as exponential decay from the vacuum-superconducting interface, $n_{\rm imp}(x) = n_0 \exp{(-x/\zeta)}$; or equivalently a local scattering rate of the form,

$$\gamma(x) = \gamma_0 e^{-x/\zeta},\tag{7}$$

where γ_0 denotes the impurity scattering rate at x=0 and ζ is the impurity diffusion length. Similar results are obtained based on a Gaussian diffusion layer. This model qualitatively captures the impurity distribution in Nitrogen treated SRF cavities, i.e. high impurity concentration near the surface and very low impurity concentration in the bulk [7]. We confine our analysis to diffusion lengths that are large compared to the coherence length, $\zeta \gg \xi$, so that we can evaluate the propagator with the locally homogeneous solution in Eq. (1). In this model the condensate momentum first reaches the critical value at the surface, i.e., the superheating condition is given by $p_s(0) = p_c(0)$, where $p_c(0)$ is the critical condensate momentum determined by the maximum scattering rate, γ_0 .

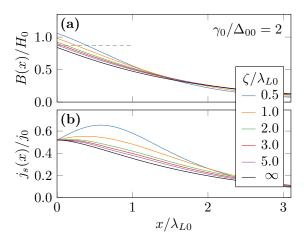


FIG. 2. The magnetic field and current density profiles, B(x) and $i_s(x)$, at the superheating field for temperature T=0, various impurity diffusion lengths ζ shown in the legend, and surface scattering rate $\gamma_0/\Delta_{00}=2$, where $\Delta_{00} = 1.78 T_c$ is the zero-temperature BCS gap in the clean limit. Panel (a): B(x) in units of the zero-temperature, clean limit critical field, $H_0 = \sqrt{4\pi N_f \Delta_{00}^2}$. The superheating field $H_{\rm sh} = B(0)$ increases with decreasing diffusion length ζ , and exceeds the superheating field for the case of homogeneous disorder with scattering rate γ_0 (dashed line). Panel (b): $j_s(x)$ in units of the zero-temperature, clean-limit critical current, $j_0 = e \, n \, \Delta_{00}/p_f$. The current density builds up away from the surface as ζ decreases, leading to larger total screening currents (the area under the curves) and thus higher superheating fields.

Results — Figure 2 shows the magnetic field and current density profiles at the superheating field for a scattering rate at the surface, $\gamma_0/\Delta_{00}=2$, where Δ_{00} is the excitation gap at T=0 in the clean limit. We present results for impurity diffusion lengths ranging from the homogeneous limit, $\zeta \to \infty$, to $\zeta/\lambda_{L0}=0.5$, scaled in units of the clean-limit, T=0, zero-field London penetration depth, $\lambda_{L0}=1/(8\pi e^2 v_f^2 N_f/3c^2)^{\frac{1}{2}}$, but restricted to $\zeta\gg\xi_0$. Fig. 2(a) shows that the superheating field, given by the field at x=0, increases with decreasing impurity diffusion length, and exceeds the absolute maximum superheating field of $H_{\rm sh}^\infty\approx0.88\,H_0$ reported in Ref. [2] for homogeneous disorder with $\gamma_0/\Delta=0.3$ (shown as the dashed line). Our analysis also confirms the prediction of Ref. [2] for the effect of homogeneous disorder.

To understand how an inhomogeneous impurity distribution leads to an increase in the superheating field consider the current density profiles shown in Fig. 2(b). At the superheating field the current density at x=0 is equal to the local critical current density, which is determined by γ_0 in each case. However, away from the surface a shorter impurity diffusion length results in a reduced impurity density and therefore larger current density for a given value the local condensate momentum. Indeed for sufficiently short impurity diffusion lengths the current density peaks at a finite distance from the vacuum-superconductor interface, resulting in a larger integrated screening current, $J=\int_0^\infty dx\, j(x)$, more effective screening of the field, and thus a higher superheating field.

Figure 3 shows the magnetic field and current density profiles at the superheating field for a fixed impurity diffusion length $\zeta/\lambda_{L0} = 1$, for a range of maximum impurity scattering rates γ_0 . In Fig. 3(a) the magnetic field pen-

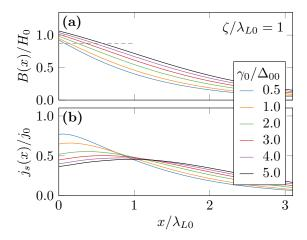


FIG. 3. Similar plots as Fig. 2, but for a fixed impurity diffusion length of $\zeta/\lambda_{L0}=1$ as a function of surface scattering rate, γ_0 , shown in the legend. The superheating field, $H_{\rm sh}=B(0)$, exceeds the theoretical maximum for the case of homogeneous disorder [2] (dashed line) over the whole range of γ_0

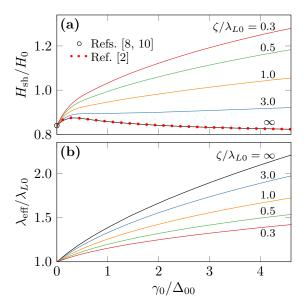


FIG. 4. The superheating field, $H_{\rm sh}$, and effective penetration depth, $\lambda_{\rm eff}$, in superconductors with an impurity diffusion layer [Eq. (7)] as functions of the surface scattering rate, γ_0 , for various impurity diffusion lengths, ζ , shown in the legend. We compare our results for the superheating field with previous calculations in the clean limit [8, 10] (black open circle) and for homogeneous disorder [2] (red circles).

etrates deeper into the superconductor with increasing impurity scattering at the surface, and the superheating field increases above the absolute maximum superheating field for homogeneous disorder [2] (dashed line). The screening current penetrates deeper further into the superconductor, but is suppressed for $x \lesssim \lambda_{L0}$, as shown in Fig. 3(b). However, the local suppression of the current near the surface is overcompensated by the increase in the screening current for $x \gtrsim \lambda_{L0}$ over a longer effective penetration depth, leading to an increase in the superheating field.

Figure 4 summarizes our results for the superheating field in impurity diffusion layers at T=0. Disorder affects the superheating field via two competing mecha-

nisms. First, the effective penetration depth, defined as

$$\lambda_{\text{eff}} \equiv B(0)^{-1} \int_0^\infty dx \, B(x) \,, \tag{8}$$

increases with disorder as shown in Fig. 4(b). As a result, the screening current penetrates deeper into the superconductor, increasing the total screening current, and as a result the superheating field. Second, impurity scattering suppresses the critical current and superheating field, c.f. Fig. 1(a). For homogeneous disorder the increase in the effective penetration depth is dominant at low scattering rates, while the suppression of supercurrent dominates at higher scattering rates. As a result the superheating field develops a peak at a relatively modest level of disorder, $\gamma_0/\Delta_{00} \approx 0.3$ shown in Fig. 4(a) for $\zeta/\lambda_{L0} = \infty$, with $H_{\rm sh} \approx 0.87 H_0$. However, in impurity diffusion layers the suppression of supercurrent is confined to the region near the surface $x \lesssim \zeta$, while due to a longer effective penetration depth [c.f. Fig. 3(b)], the screening current shifts to the relatively clean region with $x \gtrsim \zeta$. This results in a superheating field that increases with the surface scattering rate, as shown in Fig. 4(a) for diffusion lengths $\zeta/\lambda_{L0} \gtrsim 3.0$.

We note that our analysis for the superheating field based on the local critical depairing current is equivalent to the stability analysis of the Meissner state presented in Refs. [2, 8, 10]. Indeed our results agree with the previous calculations based on analyses of the thermodynamic potential. In particular we obtain $H_{\rm sh}/H_0 \approx 0.84$ for clean type-II superconductors as reported in Refs. [2, 8, 10] (black open circle in Fig. 4(a)). Our results also agree with those of Ref. [2] for the limit of homogeneous disorder, shown as the red data points in Fig. 4(a).

So far we have considered the extreme type-II limit with $\kappa^{-1} = \xi/\lambda_L \to 0$. Niobium, the material of choice for SRF applications, is marginally type II in the clean limit with $\kappa \approx 1$ [11–13]. Cavity-grade Niobium has surface disorder, and is treated with Nitrogen impurities to increase performance, both of which increase the GL parameter, thus suppressing the corrections to our theory which are of order κ^{-2} , as shown in the Appendix. Thus, we believe this work provides new insight into the role of inhomogeneous disorder on the superheating field in Nitrogen-infused Niobium SRF cavities. Moreover, our results have implications for the other superconducting materials considered for SRF applications, such as Nb₃Sn and MgB₂, both of which are strong type-II superconductors with $\kappa \gtrsim 20$ [14, 15].

Summary and Outlook — We report a theoretical investigation based on microscopic theory of inhomogeneous superconductors of the effects of impurity diffusion layers on the superheating field of superconducting RF cavities, the limiting magnetic field beyond which the Meissner state is unstable. A key result is that the introduction of an impurity diffusion layer, for example by Nitrogen infusion into Niobium, can increase the superheating field of SRF cavities above the maximum allowed superheating field predicted for the homogeneous disorder model [2]. The underlying mechanism is the increase in screening current resulting from increased field penetration depth which overcompensates suppression of Meissner current in the relatively thin dirty region near the surface. Our results strongly suggest that the impurity diffusion layers

play a role in enhancing the maximum accelerating gradient of treated SRF cavities. Although the increase in the superheating field appears to be generic to impurity diffusion layers, the magnitude of the increase depends on specific impurity profiles, suggesting that it might be possible to further increase the superheating field by engineering disorder profiles.

Acknowledgments – We thank Anna Grassellino, Alex Romanenko, Mattia Checchin and Martina Martinello

for discussions on N-doped Niobium SRF cavities which motivated this research. The research of the authors is supported by National Science Foundation Grant PHY-1734332 and the Northwestern-Fermilab Center for Applied Physics and Superconducting Technologies. This work was finalized at the Aspen Center for Physics, which is supported by National Science Foundation grant PHY-1607611.

Appendix: Long wavelength expansion of the Eilenberger Transport Equations

We solve Eilenberger's transport equation as an expansion in the ratio of length scales, $\epsilon = \{\xi/\lambda_L, \xi/\zeta\}$, for the Meissner state of inhomogeneous type-II superconductors with an impurity diffusion layer. The propagator to zeroth order in ϵ is the local solution given in Eq. (1). We also show that the leading order corrections to our calculations for the superheating field are smaller by a factor of $\epsilon^2 \sim \kappa^{-2}$.

We take the superfluid momentum to be along the y axis. The quasiclassical transport equation is then [9],

$$\left[(\varepsilon - p_s(x)v_y) \,\widehat{\tau}_3 - \widehat{\Sigma}(\varepsilon, x), \,\widehat{\mathfrak{G}}(\hat{\mathbf{p}}, \varepsilon, x) \right] + i\hbar v_x \partial_x \,\widehat{\mathfrak{G}}(\hat{\mathbf{p}}, \varepsilon, x) = 0,$$
(9)

where $v_x = v_f \hat{p}_x$, $v_y = v_f \hat{p}_y$. Spatial dependences enter via the condensate momentum, $p_s(x)$, and the impurity self energy, $\hat{\Sigma}(\varepsilon, x)$, which vary on the characteristic length scales, λ_L and ζ , respectively. We consider $\zeta \sim \lambda_L \ll \xi$, where the coherence length is $\xi = \hbar v_f/(2\pi T_c)$, and introduce the dimensionless distance, $s = x/\lambda_L$, in which case derivatives of order $\partial_s \sim O(1)$. The scaled transport equation becomes,

$$(2\pi T_c)^{-1} \left[(\varepsilon - v_f \hat{p}_y p_s(s)) \, \hat{\tau}_3 - \widehat{\Sigma}(\varepsilon, s), \, \widehat{\mathfrak{G}}(\hat{\mathbf{p}}, \varepsilon, s) \right] + i\kappa^{-1} \hat{p}_x \partial_s \widehat{\mathfrak{G}}(\hat{\mathbf{p}}, \varepsilon, s) = 0.$$
 (10)

The terms defined by the commutator on the l.h.s. of Eq. (10) are $\sim O(1)$ since T_c is the characteristic energy scale in the superconducting state. However, the gradient term is proportional to κ^{-1} , and thus of $O(\epsilon)$.

We now expand the propagator $(\widehat{o} \to \widehat{\mathfrak{G}})$ and self-energy $(\widehat{o} \to \widehat{\Sigma})$ in the small expansion parameter ϵ ,

$$\widehat{o} = \widehat{o}^{(0)} + \epsilon \, \widehat{o}^{(1)} + \epsilon^2 \, \widehat{o}^{(2)} + \dots, \tag{11}$$

such that terms $\widehat{\mathfrak{G}}^{(i)} \sim O(1)$ and $\widehat{\Sigma}^{(i)} \sim O(T_c)$. The zeroth-order terms define the locally homogeneous equation,

$$\left[\left(\varepsilon - v_f \hat{p}_y p_s(s) \right) \widehat{\tau}_3 - \widehat{\Sigma}^{(0)}(\varepsilon, s), \widehat{\mathfrak{G}}^{(0)}(\hat{\mathbf{p}}, \varepsilon, s) \right] = 0.$$
 (12)

When combined with the Eilenberger's normalization condition, $(\widehat{\mathfrak{G}}^{(0)})^2 = -\pi^2 \widehat{1}$, we obtain the locally homogeneous propagator in Eq. (1).

The first-order correction to the propagator satisfies

$$(2\pi T_c)^{-1} \left\{ \left[(\varepsilon - v_f \hat{p}_y p_s(s)) \, \hat{\tau}_3 - \widehat{\Sigma}^{(0)}(\varepsilon, s), \, \widehat{\mathfrak{G}}^{(1)}(\hat{\mathbf{p}}, \varepsilon, s) \right] + \left[\widehat{\mathfrak{G}}^{(0)}(\hat{\mathbf{p}}, \varepsilon, s), \, \widehat{\Sigma}^{(1)}(\varepsilon, s) \right] \right\} + i \hat{p}_x \partial_s \widehat{\mathfrak{G}}^{(0)}(\hat{\mathbf{p}}, \varepsilon, s) = 0. \quad (13)$$

By separating the terms according to their symmetry under $\hat{p}_x \to -\hat{p}_x$ and noting that both $\widehat{\mathfrak{G}}^{(0)}$ and $\widehat{\Sigma}^{(0)}$ are even in \hat{p}_x , we see that the source term generates $\widehat{\mathfrak{G}}^{(1)}$ which is odd in \hat{p}_x . Consequently both pairing and (s-wave) impurity self-energies vanish since they are linear in $\langle \widehat{\mathfrak{G}}^{(1)} \rangle = 0$. Using Eq. (1), we eliminate $\widehat{\Sigma}^{(0)}$ in favor of $\widehat{\mathfrak{G}}^{(0)}$ to obtain,

$$(2\pi T_c)^{-1}(-\pi)^{-1}C^{(0)}(\hat{\mathbf{p}},\varepsilon,s)\left[\widehat{\mathfrak{G}}^{(0)}(\hat{\mathbf{p}},\varepsilon,s),\widehat{\mathfrak{G}}^{(1)}(\hat{\mathbf{p}},\varepsilon,s)\right] + i\hat{p}_x\partial_s\widehat{\mathfrak{G}}^{(0)}(\hat{\mathbf{p}},\varepsilon,s) = 0,$$
(14)

where $C^{(0)}$ is a scalar. Inverting this equation, we have

$$(-2\pi^2)(2\pi T_c)^{-1}(-\pi)^{-1}C^{(0)}(\hat{\mathbf{p}},\varepsilon,s)\widehat{\mathfrak{G}}^{(1)}(\hat{\mathbf{p}},\varepsilon,s) = -i\hat{p}_x\widehat{\mathfrak{G}}^{(0)}(\hat{\mathbf{p}},\varepsilon,s)\partial_s\widehat{\mathfrak{G}}^{(0)}(\hat{\mathbf{p}},\varepsilon,s). \tag{15}$$

In deriving the above equation we make use of the normalization conditions: $(\widehat{\mathfrak{G}}^{(0)})^2 = -\pi^2 \widehat{1}$ and $\widehat{\mathfrak{G}}^{(0)} \widehat{\mathfrak{G}}^{(1)} + \widehat{\mathfrak{G}}^{(1)} \widehat{\mathfrak{G}}^{(0)} = 0$. Finally, we show that $\widehat{\mathfrak{G}}^{(1)}$ is purely off-diagonal. To see this we note that $\widehat{\mathfrak{G}}^{(0)} = a_3 \widehat{\tau}_3 + a_1 (i\sigma_y \widehat{\tau}_1)$ and thus $\widehat{\mathfrak{G}}^{(1)} \propto \widehat{\mathfrak{G}}^{(0)} \partial_s \widehat{\mathfrak{G}}^{(0)} = b_0 \widehat{1} + b_2 (i\sigma_y \widehat{\tau}_2)$. In addition since $(\widehat{\mathfrak{G}}^{(0)})^2 = -\pi^2 \widehat{1}$, we have $\operatorname{tr} \widehat{\mathfrak{G}}^{(1)} = \operatorname{tr} \widehat{\mathfrak{G}}^{(0)} \partial_s \widehat{\mathfrak{G}}^{(0)} = 0$. As a result $\widehat{\mathfrak{G}}^{(1)} \propto i\sigma_y \widehat{\tau}_2$. That is, $\widehat{\mathfrak{G}}^{(1)}$ does not contribute to the transport current, so the leading corrections to our results for the superheating field are of order $\epsilon^2 \sim \kappa^{-2}$.

[†] sauls@northwestern.edu

^{*} wave@northwestern.edu

- C. P. Bean and J. D. Livingston, Phys. Rev. Lett. 12, 14 (1964).
- [2] F. P.-J. Lin and A. Gurevich, Phys. Rev. B 85, 054513 (2012).
- [3] A. Gurevich, AIP Adv. 5, 017112 (2015).
- [4] D. B. Liarte, M. K. Transtrum, and J. P. Sethna, Phys. Rev. B 94, 144504 (2016).
- [5] D. B. Liarte, S. Posen, M. K. Transtrum, G. Catelani, M. Liepe, and J. P. Sethna, Supercond. Sci. Tech. 30, 033002 (2017).
- [6] T. Kubo, Supercond. Sci. Tech. 30, 023001 (2017).
- [7] A. Grassellino, A. Romanenko, Y. Trenikhina, M. Checchin, M. Martinello, O. S. Melnychuk, S. Chandrasekaran, D. A. Sergatskov, S. Posen, A. C. Crawford, S. Aderhold, and D. Bice, Supercond. Sci. Tech. 30, 094004 (2017).

- [8] G. Catelani and J. P. Sethna, Phys. Rev. B 78, 224509 (2008).
- [9] G. Eilenberger, Zeit. f. Physik **214**, 195 (1968).
- [10] V. P. Galaiko, Sov. Phys. JETP 23, 745 (1966).
- [11] T. F. Stromberg and C. A. Swenson, Phys. Rev. Lett. 9, 370 (1962).
- [12] B. W. Maxfield and W. L. McLean, Phys. Rev. 139, A1515 (1965).
- [13] D. K. Finnemore, T. F. Stromberg, and C. A. Swenson, Phys. Rev. 149, 231 (1966).
- [14] T. P. Orlando, E. J. McNiff, S. Foner, and M. R. Beasley, Phys. Rev. B 19, 4545 (1979).
- [15] B. B. Jin, N. Klein, W. N. Kang, H.-J. Kim, E.-M. Choi, S.-I. Lee, T. Dahm, and K. Maki, Phys. Rev. B 66, 104521 (2002).